ENVIRONMENTAL FIELD ESTIMATION BY CONSENSUS BASED DYNAMIC SENSOR NETWORKS AND UNDERWATER GLIDERS

Raffaele Grasso[*], *Paolo Braca*[*], *Stefano Fortunati*[#§], *Fulvio Gini*[#§], *Maria S. Greco*[#§]

[*]STO Centre for Maritime Research and Experimentation (CMRE), Viale San Bartolomeo 400, 19126 La Spezia, Italy, {Raffaele.Grasso, Paolo.Braca}@cmre.nato.int

[#]Dept. of Information Engineering, University of Pisa, Italy, [§]CNIT RaSS (Radar and Surveillance System) National Laboratory, Pisa, Italy, {stefano.fortunati, m.greco, f.gini}@iet.unipi.it

ABSTRACT

A coordinated dynamic sensor network of autonomous underwater gliders to estimate 3D time-varying environmental fields is proposed and tested. Each sensor performs local Kalman filter sequential field estimation. A network of surface relay nodes and asynchronous consensus are used to distribute local information among all nodes so that they can converge to an estimate of the global field. Tests using data from real oceanographic forecast models demonstrate the feasibility of the approach with relative error performance within 10%.

Index Terms—Sensor networks, consensus, distributed estimation, autonomous underwater vehicles.

1. INTRODUCTION

This work describes a distributed algorithm to estimate 3D slowly varying environmental spatial fields (such as sea water temperature) by a fleet of autonomous underwater gliders (agents) equipped with sensors that acquire field measurements [1][2]. It is assumed that direct communications between agents are not possible. An agent can sporadically emerge and communicate with a surface node to transfer information. The decentralization of the estimation algorithm is achieved by integrating the fleet with a network of surface relay nodes (RNs) communicating with the agents by satellite/radio links. The RNs act as information gateways to asynchronously distribute the local information collected by one sensor to all the others. The global estimation of the spatial field is, in this way, iteratively computed and somehow shared by all the nodes of the network. The estimated field is retrieved by interrogating a node when this is reachable by the user.

The network is characterized by a random switching topology with asynchronous communications. The information diffusion is based on the asynchronous consensus protocol among sensors and the RNs [3], [4], [5], [6]. The network sampling strategy is adaptive: the path of an agent of the network is optimized so that the agents are forced to move into the most informative regions, where the estimate is more inaccurate [7].

The architecture is suitable for large-scale networks of autonomous underwater gliders (AUGs), a vehicle that flies through the ocean by controlling its buoyancy [1]. These vehicles typically perform underwater missions covering large areas and for long periods of time (even months). They form a multi-payload platform carrying on board several scientific sensors at the same time such as conductivity, temperature and depth (CTD) sensors, seawater optical parameter sensors and acoustic hydrophones. They can communicate to a command and control center through a satellite/radio link only when at sea surface and cannot communicate underwater with other vehicles or gateways at very long range through an acoustic link due to energy budget and communication equipment constraints. Moreover, due to environmental factors, surfacing phases of the agents cannot be easily synchronized.

This work is based on the seminal papers [8] and [9] on spatial field distributed estimation by centralized as well as decentralized dynamic sensor networks. The papers do not take into account networks with intermittent communication links. The novel contribution of this paper consists in the design and the application of an adaptive dynamic network for 3D ocean field estimation in a distributed way by a fleet of AUGs exchanging information asynchronously through the RN network. The paper aims at evaluating the performance of the system for some specific scenarios. The scenario here reported is based on a real 3D oceanographic forecast model of the seawater temperature, the Navy Coastal Ocean Model (NCOM) [10]. The achieved mean steady state relative error between the estimated and the true field is within 10%.

The paper is organized as follows. Section 2 provides the overview of the system, including single agent Kalman filter (KF) estimation, agent control law, and a simple kinematic model of the glider. In Sect. 3, the consensus protocol is detailed. Section 4 provides simulation results while Sect. 5 draws conclusions and gives ideas for future work.

2. AGENT LOCAL ESTIMATION

This section provides an overview of the local field estimation algorithm performed by each sensor. The estimation procedure relies on the expansion of the spatial field on a basis of known spatial functions, weighted by unknown coefficients, which are in general time variant. The

978-0-9928626-3-3/15/$31.00 ©2015 IEEE

spatial field to be estimated can be written as [8]:

$$g(\mathbf{r},t) = \Psi(\mathbf{r})^T \mathbf{c}(t) = \sum_{j=1}^{L} c_j(t)\psi_j(\mathbf{r}), \qquad (1)$$

where $\mathbf{r}$ is the coordinate vector of the region of interest, t is the time variable, $\mathbf{c}(t) = [c_1(t),...,c_L(t)]^T$ is the real coefficient vector and $\Psi(\mathbf{r}) = [\psi_1(\mathbf{r}),...,\psi_L(\mathbf{r})]^T$ is the vector of the base functions at a given position $\mathbf{r}$. Given the base vector, $\Psi(\mathbf{r})$, the problem of estimating the scalar field, $g(\mathbf{r},t)$, is equivalent to estimate the coefficient vector $\mathbf{c}(t)$. In this work, we assume that the coefficient vector is constant or slowly time-varying, *i.e.* $\mathbf{c}(t) \approx \mathbf{c}$. The base functions in (1) are assumed to be of the radial type. In particular, a set of Gaussian-like radial basis functions (RBF), $\psi_j(\mathbf{r}) = \exp(-||\mathbf{r}-\mathbf{r}_j||^2/\beta)$, is chosen with a given spread parameter β (constant for all the functions) and centers $\mathbf{r}_j$ located on a regular grid in the spatial region of interest.

The agent local sequential estimation of the field is performed by a Kalman filter in which the coefficient dynamic is modeled by a linear state space equation shared by all the agents (AUGs) in the network:

$$\mathbf{c}_{i,k} = \mathbf{c}_{i,k-1} + \mathbf{n}_{i,k}, \qquad (2)$$

where $\mathbf{n}_{i,k}$ are Gaussian distributed independent noise vectors with covariance matrix $\mathbf{Q}_{i,k} = \mathrm{diag}(\sigma^2_{1,i,k},...,\sigma^2_{L,i,k})$. The matrix $\mathbf{Q}_{i,k}$ is a free parameter that can be tuned to adjust the velocity at which the system adapts its estimate to the true dynamic of the coefficients [11]. The tradeoff to be considered is between filtering response of the system and estimate residual error [11].

Assuming a network composed of N sensors, the i-th sensor, for i=1,…,N, acquires at each time step a noisy measurement $y_{i,k}$ of the field. According to (1), the measurement equation of the i-th sensor can be expressed as follows:

$$y_{i,k} = \Psi(\mathbf{p}_{i,k})^T \mathbf{c}_{i,k} + e_{i,k}, \qquad (3)$$

where $\mathbf{p}_{i,k}$ is the position vector of the i-th sensor at time step k and $e_{i,k}$ is the scalar Gaussian measurement noise, independent from $\mathbf{n}_{i,k}$, with zero-mean and variance $\rho^2_{i,k}$. Each sensor runs the Kalman filter prediction and update steps to provide the sequential estimate, $\hat{\mathbf{c}}_{i,k}$, of the coefficient vector and its covariance matrix, $\hat{\mathbf{C}}_{i,k}$, to an RN.

3. DISTRIBUTED CONSENSUS ALGORITHM

This section describes how local estimates from each network agent can be exploited to achieve global field estimation in a distributed way. The resulting network architecture has a switching topology [12] and is based on the consensus paradigm in which the information is diffused among the agents through the RNs that act as information gateways.

In the proposed network model, agents can communicate with a RN at random instants but cannot communicate among each other. Each agent sequentially estimates the coefficient vector by means of a KF from local field measurements and updates its position applying a control law by using the local prediction of the coefficient estimate covariance matrix (see Section 4). An agent transmits its local coefficient vector estimate and covariance to a connected RN when at surface (no field measurements are provided to RNs). The RN distributes its estimates (coefficient vector and covariance) to the other RNs and to the connected agents. The RN updates its estimates through the average consensus algorithm ([4], [5]) by combining the local agent's estimates, when available, and the estimates received by the other RNs. Agents connected to an RN update their local estimates through the average consensus by fusing the RN estimates with the local ones.

The protocol allows the global information to intermittently flow into the network through RNs and at the same time promotes a collaborative behavior among agents. Realistic numerical simulations show that agent and RN estimates statistically converge to the true global coefficient vector reaching the consensus.

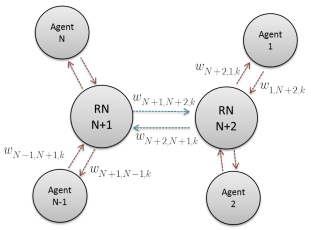

Fig. 1. Star network topology with time varying link weights.

The network of agents and RNs are modeled as an undirected graph with the topology in Figure 1. The whole network has a set of $N+N_r$ nodes, $\mathrm{N} = \{1,2,...,N+N_r\}$, with $\{N,...,N+N_r\}$ being the indices of the RNs, and an adjacency matrix given by:

$$\mathbf{A} = \begin{bmatrix} \mathbf{I}_{N\times N} & \mathbf{1}_{N\times N_r} \\ \mathbf{1}^T_{N\times N_r} & \mathbf{1}_{N_r\times N_r} \end{bmatrix} \qquad (4)$$

which defines the set of all possible graph edges $\varepsilon = \{(i,l) \mid A_{i,l} = 1,\ i,l \in \mathrm{N}\}$ ($\mathbf{I}_{N\times N}$ is the $N\times N$ identity matrix, while $\mathbf{1}_{N\times N_r}$ and $\mathbf{1}_{N_r\times N_r}$ are the $N\times N_r$ and $N_r\times N_r$ matrix of all ones, respectively). If the topology is fixed, the graph in (4) is strongly connected. Actually, the structure of the network is dynamic *i.e.* at each time step *k,* there is a subset $\varepsilon_k \subseteq \varepsilon$ of edges which are active, where an edge $i,l \in \varepsilon_k$ is active if node i can communicate with node l. The i-th node applies the consensus algo-

rithm as follows:

$$\hat{\mathbf{g}}_{i,k} = \sum\nolimits_{l \in \mathrm{N}_{i,k}} w_{i,l,k} \hat{\mathbf{g}}_{l,k} \,, \tag{5}$$

$$\hat{\mathbf{D}}_{i,k} = \sum\nolimits_{l \in \mathrm{N}_{i,k}} w_{i,l,k} \hat{\mathbf{D}}_{l,k} \,, \tag{6}$$

where $\hat{\mathbf{D}}_{\cdot,k} = \hat{\mathbf{C}}_{\cdot,k}^{-1}$ is the information matrix, $\hat{\mathbf{g}}_{\cdot,k} = \hat{\mathbf{D}}_{\cdot,k} \hat{\mathbf{c}}_{\cdot,k}$ is the information vector, $\mathrm{N}_{i,k}$ is the set of node neighbors of the *i*-th node at time step *k* (the node *i* is included in the set) and $w_{i,l,k}$ are weighting parameters. Once the consensus has been applied, the updated coefficient estimate and the associated covariance for the *i*-th node are $\hat{\mathbf{c}}_{i,k} = \hat{\mathbf{D}}_{i,k}^{-1} \hat{\mathbf{g}}_{i,k}$ and $\hat{\mathbf{C}}_{i,k} = \hat{\mathbf{D}}_{i,k}^{-1}$, respectively. The fusion rules (5) and (6) are used in the so called information consensus filter [13] and are optimum in the minimum mean square error (MMSE) and maximum likelihood (ML) sense in the case the sensor estimates are independent [14]. As this hypothesis is not always true, the fusion rule is in general sub-optimal, but with the advantage of having a reduced complexity. The choice of the weights in the consensus update is crucial for guaranteeing certain properties and asymptotic convergence. In particular, in this work, the Metropolis weights are considered:

$$w_{i,l,k} = \begin{cases} 1 / \left[1 + \max\left(d_{i,k}, d_{l,k} \right) \right] & \left(i,l \right) \in \varepsilon_k \\ 1 - \sum\limits_{l \in \mathrm{N}_{i,k} \setminus i} w_{i,l,k} & i = l \\ 0 & \text{otherwise} \end{cases}, \tag{7}$$

with $d_{i,k} = |\, \mathrm{N}_{i,k} \,|$ the cardinality of $\mathrm{N}_{i,k}$. This choice is average preserving and for certain problems of distributed consensus, it provides asymptotic convergence to a global solution under mild conditions on the sequence of sets of active edges ε_k.

The consensus update phase is completely asynchronous in the sense described in [17]. The *i*-th field sensor applies consensus if it is connected to an RN at $k=k_i$. With the given network topology, the direct communication between glider agents is not possible. However, sensors indirectly combine their estimates among each other through RNs. The estimate at RNs allows the diffusion of the information through the network and the convergence of any local agent estimates to the global statistic. At the same time, the glider applies correction to the navigation heading according to the control law in Sect. 4. The next update (*i.e.* the next glider surfacing) is at $k_i+\Delta_i$ where Δ_i is a random variable with a given distribution. The switching topology of the network is determined by the fact that a glider cannot communicate during the underwater phase. The surface phases of the gliders, and by consequence communications and dynamic control, cannot be synchronized in a practical way, determining the asynchrony [15] of the whole system and the randomness of the adjacency matrix of the network. The distribution of Δ_i is used to model asynchrony and connectivity randomness, and determines the probability law of the time varying adjacency matrix and the degree of convergence of each network node to the global solution. In this work, a glider comes at surface independently from the other ones and Δ_i has a uniform discrete distribution, with parameters as specified in Sect. 5. A deeper insight into the convergence properties of consensus algorithms in asynchronous and switching topology networks can be found in [12][15][16][18][19]. In the switching topology case, if the union of the connectivity graphs in the observation interval is strongly connected, the consensus algorithm asymptotically converges to the true solution as demonstrated in [18].

4. NETWORK CONTROL

Following [8], the local sensor control is obtained by updating the next agent positions to minimize the average predicted covariance of the scalar field estimate. Using the coefficient covariance matrix from the KF, this quantity is given by:

$$J = \int_A \Psi\left(\mathbf{r}\right) \hat{\mathbf{C}}_{k|k-1} \Psi^T\left(\mathbf{r}\right) dA \,, \tag{8}$$

where the integration is over the area of interest, *A*, in which the agents are constrained to operate. As in [5], the position $\mathbf{p}_{i,k}$ of the *i*-th agent is given by

$$\mathbf{p}_{i,k} = \mathbf{p}_{i,k-1} + \mathbf{f}_{i,k-1} \,, \tag{9}$$

where the control input $\mathbf{f}_{i,k-1}$ is implemented by a gradient control law as follows:

$$\mathbf{f}_{i,k-1} = -S \frac{\partial J}{\partial \mathbf{p}_{i,k-1}} \,, \tag{10}$$

where

$$\frac{\partial J}{\partial \mathbf{p}_{i,k-1}} = \int_A \Psi\left(\mathbf{r}\right) \frac{\partial \hat{\mathbf{C}}_{k|k-1}}{\partial \mathbf{p}_{i,k-1}} \Psi^T\left(\mathbf{r}\right) dA \,, \tag{11}$$

and *S* is a constant gain (see [8] for the details of the control law calculation given the base functions). In general, the control law (9) can also include a repulsive potential additive term to provide a good covering of the area to be explored and to avoid collisions among agents. This term requires the knowledge of the position of the other agents that can be provided through the RN network. Obviously, the network state at a given time step can be partially known to an agent due to the asynchrony of the system. The impact of this on the overall system performance will be investigated in future works.

The dynamic of the agents in (9) is adapted, as specified below, to model the kinematic of an AUG that navigates at a constant speed (in absence of sea current) with a constrained vertical plane dynamic and a waypoint guidance system. Generally, a glider moves through a 3D space following a saw-tooth shape trajectory (see Fig. 2) in the vertical plane. The trajectory is composed of a certain number of dive/climb cycles in the interval between two surfacing phases of the glider. The information, col-

lected during each dive/climb cycle, is stored and finally transmitted during the surfacing phase.

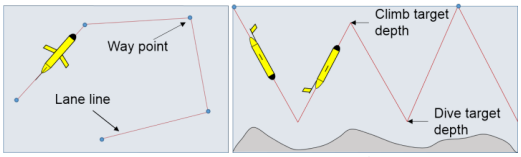

Fig. 2. Glider mission plan: a) way points and lane lines in the horizontal plane, and b) yo-yo trajectory in the vertical plane.

The glider dynamic model considered in this work assumes a constant velocity without water current disturbances, constrained to follow a yo-yo trajectory in the vertical plane with given climbing and diving target depths [15]. The glider navigates in the vertical plane along a yo-yo segment with a given pitch angle ϕ. The control vector (10) is normalized and multiplied by the total glider speed V to take into account the constant speed constraint:

$$\tilde{\mathbf{f}}_{i,mB} = V\mathbf{f}_{i,mB} / \| \mathbf{f}_{i,mB} \| . \qquad (12)$$

The 2D components of the control law (9) are applied at each glider surfacing to optimally change the vehicle direction in the horizontal plane.

5. NUMERICAL ANALYSIS

The system is tested by simulating one RN and a network of underwater gliders equipped with seawater temperature sensors. The true field is a series of consecutive 3D forecasts of sea water temperature (with 3h sampling period) of the Navy Coastal Ocean Model [10], spanning an observation period of 7 days. The model was provided by the Naval Research Laboratory-Stannis Space Centre (NRL-SSC), during the STO-CMRE 2011 Recognized Environmental Picture cruise trial (REP11) in the Mediterranean Sea. The data set used in the simulation represents a sub-volume of about 60 by 60 Km in the horizontal plane by 100 m along depth. The horizontal resolution is about 2 by 2 Km. The initial depth levels (not regularly spaced) have been linearly interpolated between 0 and 100 m. The resulting regular data grid has a size of 30×30×30 samples. All spatial coordinates are normalized between 0 and 1 for convenience. The basis function dictionary is of 343 Gaussian RBFs (*i.e.* the state coefficient vector **c** has 343 entries) arranged on a 7×7×7 3D regular sub-grid of the original 30×30×30 NCOM model grid. The RBF covariance matrix is $\mathbf{V}=0.025\mathbf{I}_3$, constant for all the dictionary functions. The RBF spread parameter was chosen empirically by roughly estimating the spatial scale of the main oceanographic features present in the data. The measurement equation of each agent is (3) with measurement noise variance $\rho_k^2=0.001$. The network includes N=15 AUGs with agent speed of 0.6 m/s, pitch angle equal to ϕ=26° and sampling rate of T=6 s. The time delay between adjacent surfacing phases of an agent is modeled as a uniform random variable, $\Delta \sim U(\eta-\delta, \eta-\delta)$, to take into account random fluctuations due to unknown environmental conditions affecting the agent navigation. The average delay η is typically between 1-3 hours. δ is set to 15 min as estimated from a set of real AUG navigational data.

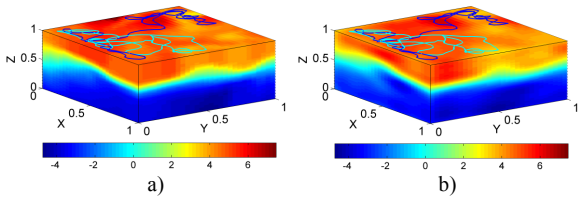

Fig. 3. a) NCOM sea water temperature field variations (in °C) after 7 days and b) reconstructed field (with vehicle tracks).

Fig. 3-a) shows an example of the true NCOM field at the end of the observation period. Without loss of generality, the spatial/temporal mean of the field has been subtracted from the original data set. Fig. 3-b) presents the 3D view of the reconstruction of the field at the end of the observation period showing a good match with the true field in terms of main oceanographic features both in the horizontal plane and along the vertical water column. The results are for η=1h.

Fig. 4-a) shows vertical profiles of the true NCOM field along the trajectory of the agent 1 while Figure 4-b depicts the estimated profile by the same agent. The main oceanographic features are well resolved as well as the thermocline separating water masses with different characteristics.

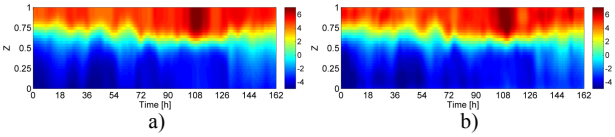

Fig. 4. a) NCOM sea water temperature field vertical profile along agent 1 track; b) estimated field along the same tracks.

Fig. 5-a) shows sensor and RN field estimates versus time (sub-sampled every 3 hours) for a given spatial position (x=0.79, y=0.66, z=1.00) compared with the true field (in green). The system starts to track the field variations after a transition phase of about 18 hours. Fig. 5-b) shows the spatial field RMSE versus time for different values of N and η. The graph can provide some indications about the best parameters to be used in a real scenario (having the same time/spatial scale and variability as the simulated one) in order to achieve the best possible performance at an affordable cost (with respect to the number of sensors and number of transmissions in the observation period).

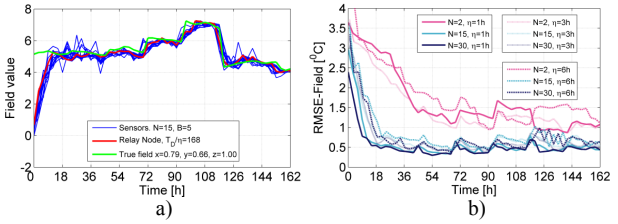

Fig. 5. a) Sensors and RNs estimated field at a given position, sub-sampled every 3 hours. b) Field RMSE versus time.

In particular, the number of sensors significantly affects

the error and the adaptation capability of the system for $N<15$. For $N\geq15$, at steady state, the network adaptation allows the network to keep the RMSE value close to 0.5 ^{o}C with η that does not significantly affect the performance. The spatial percentage error of the field after the transitory phase and for $N\geq15$ is close to 10%.

6. CONCLUSIONS

In this paper, a coordinated dynamic sensor network of autonomous underwater gliders to estimate oceanographic 3D spatial scalar fields is proposed and tested on realistic scenarios. Each agent performs the local estimation of the field statistics by a KF that processes local field measurements. The local estimates of an agent are updated through an asynchronous consensus algorithm, exploiting the local estimates of the others so that all nodes converge on average to the true global field. The asynchronous information exchange and fusion is handled by a subnetwork of RNs communicating with agents at surface. An agent uses updated estimates to locally control its position and acquire field measurements in the most informative areas and adaptively track field variations.

The system has been tested on scenarios built on real oceanographic forecast models. The scenario here presented simulates a glider fleet mission of 7 days using 3D time-varying seawater temperature data provided by the NCOM forecast model for a Mediterranean Sea area, in the framework of the REP11 experiment. For typical fleet operational parameters (*i.e.* 15 agents and 1-3 hours surfacing period) and surveyed area size (60×60 Km horizontally and 100 m vertically) the average performance achieved in terms of relative error at steady state is within 10%, showing good qualitative convergence and tracking properties.

Future work includes: i) the on-line estimation of base functions unknown parameters, such as the mean and the covariance of Gaussian RBFs, ii) an investigation on the effects of the water current on the agent navigation and iii) an in depth investigation on the algorithm convergence and convergence rate properties [18][19].

ACKNOWLEDGMENT

NCOM forecasts are provided by the US Naval Research Laboratory–Stennis Space Center (NRL-SSC). This work has been funded by the NATO Allied Command Transformation (NATO-ACT) under the project ACT000405, Environmental Knowledge and Operational Effectiveness–Decisions in Uncertain Ocean Environments (EKOE-DUOE).

7. REFERENCES

[1] Schofield, O., J. Kohut, D. Aragon, L. Creed, J. Graver, C. Haldeman, J. Kerfoot, H. Roarty, C. Jones, D. Webb, and S.M. Glenn., "Slocum gliders: Robust and ready," *Journal of Field Robotics* 24(6):1–14, 2007.

[2] Paley, D.A., Fumin Zhang, Leonard, N.E., "Cooperative Control for Ocean Sampling: The Glider Coordinated Control System," *IEEE Transactions on Control Systems Technology,* vol.16, no.4, pp.735,744, July 2008, doi: 10.1109/TCST.2007.912238.

[3] Olfati-Saber, R.; Fax, J.A.; Murray, R.M., "Consensus and Cooperation in Networked Multi-Agent Systems," *Proceedings of the IEEE*, vol.95, no.1, pp.215-233, Jan. 2007.

[4] P. Braca, S. Marano, V. Matta and P. Willett, "Asymptotic Optimality of Running Consensus in Testing Binary Hypotheses," *IEEE Transactions on Signal Processing*, vol.58, no.2, pp.814,825, Feb. 2010.

[5] P. Braca, S. Marano, and V. Matta, "Enforcing Consensus While Monitoring the Environment in Wireless Sensor Networks," *IEEE Transactions on Signal Processing*, vol. 56, no. 7 pp.3375,3380, July 2008.

[6] Kar, S.; Moura, J.M.F., "Consensus + innovations distributed inference over networks: cooperation and sensing in networked systems," *IEEE Signal Processing Magazine,* vol.30, no.3, pp.99-109, May 2013.

[7] P. Braca, R. Goldhahn, K. LePage, S. Marano, V. Matta and P. Willett, "Cognitive Multistatic AUV Networks," *in Proc. of the 17th International Conference on Information Fusion (FUSION 2014)*, Salamanca 2014.

[8] K. M. Lynch et al, "Decentralized Environmental Modeling by Mobile Sensor Networks," *IEEE Transactions on Robotics*, Vol. 24, No 3, June 2008.

[9] Hung Manh La; Weihua Sheng, "Distributed Sensor Fusion for Scalar Field Mapping Using Mobile Sensor Networks," *IEEE Transactions on Cybernetics*, vol.43, no.2, pp.766, 778, April 2013.

[10] Martin, P. J., "A description of the Navy Coastal Ocean Model Version 1.0," NRL Rep. NRL/FR/7322– 00–9962, 42 pp., NRL, Stennis Space Center, MS, USA, 2000.

[11] Julier, S., J., Uhlmann, J., K., "Unscented Filtering and Nonlinear Estimation," *Proceedings of the IEEE*, Vol. 92, No. 3, March 2004.

[12] Olfati-Saber, R.; Murray, R.M., "Consensus problems in networks of agents with switching topology and time-delays," *IEEE Transactions on Automatic Control,* vol.49, no.9, pp.1520-1533, Sept. 2004.

[13] Xie Li, Huang Caimou, and Hu Haoji, "Distributed Filter with Consensus Strategies for Sensor Networks," *Journal of Applied Mathematics*, vol. 2013, Article ID 683249, 9 pages, 2013. doi:10.1155/2013/683249.

[14] Chang, K., C.; Saha, R., K.; Bar-Shalom, Y., "On Optimal Track to-Track Fusion," IEEE Transactions on Aerospace and Electronic Systems, vol. 33, no. 4, Oct. 1997.

[15] Xiaoa, F., Wanga, L., "State consensus for multi-agent systems with switching topologies and time-varying delays," *International Journal of Control*, vol. 79, issue 10, pp 1277-1284, 2006, doi: 10.1080/00207170600825097.

[16] Grasso R, Cecchi D, Cococcioni M, Trees C, Rixen M, Alvarez A, Strode C, "Model based decision support for underwater glider operation monitoring," *Proceedings OCEANS 2010 MTS/IEEE*, Seattle. pp. 1–8, 2010.

[17] Jiahu Qin, Changbin Yu, Hirche, S., "Stationary Consensus of Asynchronous Discrete-Time Second-Order Multi-Agent Systems Under Switching Topology," *IEEE Transactions on Industrial Informatics*, vol.8, no.4, pp.986,994, Nov. 2012, doi: 10.1109/TII.2012.2210430

[18] Kingston, D.B., Beard, R.W., "Discrete-time average-consensus under switching network topologies," American Control Conference, 14-16 June 2006, doi: 10.1109/ACC.2006.1657268.

[19] Pereira, S.S., Pages-Zamora, A., "Mean Square Convergence of Consensus Algorithms in Random WSNs," *IEEE Transactions on Signal Processing*, vol.58, no.5, pp.2866,2874, May 2010, doi: 10.1109/TSP.2010.2043140.